Morphology and Crystallization Kinetics of a Rigid Rod, Fully Aromatic, Liquid Crystalline Copolyester

D. Dainelli[†] and L. L. Chapoy*[,‡]

Himont Italia, via Caduti del Lavoro, 28100 Novara, Italy

Received February 18, 1992; Revised Manuscript Received August 10, 1992

ABSTRACT: The kinetics of the isothermal crystallization of a phenylethylhydroquinone, phenylhydroquinone, terephthalic acid nematic liquid crystalline copolyester have been studied by differential scanning calorimetry in the temperature interval 319–325 °C. The polymer is characterized by being highly crystalline in spite of its copolymeric nature. The crystallization process is describable by an Avrami equation. This polymer gives the opportunity of studying a crystallization process for chains in which the crystalline morphology is preformed, due to nematic state ordering, thereby giving a well-defined chain morphology from which to initiate crystallization. This feature can facilitate an unambiguous interpretation of the Avrami parameters.

Introduction

The kinetics of the phase transition of liquid crystalline materials has been a subject of interest in recent times. The study of the crystallization kinetics from the mesophase and/or isotropic melt can provide information regarding the nucleation process and growth of the crystal/mesophase with reference to the type and degree of order in the high temperature less ordered phase. The phase transitions of low molar mass liquid crystalline compounds, mostly cholesteric esters, have been studied.[1–5] Kinetic studies dealing with isotropic-anisotropic thermotropic phase transition of liquid crystalline polymers both pure[6,7] and blended with other thermoplastic polymers[8] can be found. In all cases the kinetics of the transition can be described in terms of the Avrami equation[9]

$$X(t) = 1 - \exp(-kt^n) \qquad (1)$$

where X is the weight fraction of crystalline component, k is a rate parameter of the crystallization process, and n is the Avrami exponent, a parameter related to the geometry and morphology of the growth. Note that the equation was originally derived in terms of the volume fraction of crystalline phase.

At present, however, only a few studies have been directed toward the crystallization kinetics of liquid crystalline polymers from the mesomorphic phase. These are of the flexible spacer type[10,11] and the main chain type.[12] The crystallization kinetics of liquid crystalline polymers containing flexible spacers will in part depend on the equilibrium conformation of the flexible spacer and the correlation time for conformational rearrangements in order to achieve a crystallizable chain conformation. They do not, therefore, make good model substances to study the crystallization of rigid rods from the nematic state.

Warner and Jaffe[13] studied a rigid thermotropic polyester composed of hydroxybenzoic acid, naphthalenedicarboxylic acid, hydroquinone, and isophthalic acid, i.e. a polymer not containing a flexible spacer. Their results were interpreted in terms of rodlike growth, indicating that the structure of the crystal closely resembles that of the nematic melt, but with the higher symmetry required by the crystalline state. However, the lack of well-developed three-dimensional crystallinity, as evidenced by the X-ray diffraction pattern and thermal analysis data, indicated a frozen-in liquid crystalline structure rather than a true crystal. It would appear, therefore, in hindsight that their data reflect the growth of highly defective paracrystals associated with nematic copolymers containing disruptive kink and crankshaft moieties.

In this paper we report results for the crystallization kinetics of a linear, rigid, wholly aromatic copolyester from the nematic state. The polymer in question is a 1:1:2 copolyester based on phenylhydroquinone, phenylethylhydroquinone, and terephthalic acid as shown in Figure 1 and has been the subject of a recent study by Cheng et al.[12] This polymer is made to be thermally tractable by the introduction of bulky lateral substituents which reduce the cohesive energy density of the crystal, thereby reducing the melting point to the 330–340 °C range. The polymer, in spite of the bulky side groups and copolymeric nature, shows a sharp, structured X-ray diffraction pattern, Figure 2A, indicative of a highly crystalline material. Evidently, the two hydroquinone moieties are isomorphic in the crystallization process allowing them to cocrystallize.[14] The isomorphic nature of the hydroquinone moieties, thus, allows the polymer to crystallize in the classical sense, i.e. a structure containing long range three-dimensional order. Cheng et al.[15] have prepared the two homopolymers and three intermediate compositions and have observed only a 15° degree variation in melting point over the whole composition range. They concluded that the two hydroquinones are randomly distributed in the chains and that a solid–solid solution is formed also in the crystalline state. In spite of the apparent complexity of this family of polymers, they appear to provide the experimental basis of a tractable rigid rod polymer. This is distinctly contrasted from the crystallization behavior usually observed in aromatic random copolyesters which by the conventional wisdom of copolymer logic should not crystallize at all or rather only to the extent that suitable blocky sequences can be brought into juxtaposition.

Examples of the latter are given by liquid crystalline copolyesters which gain their tractability through the introduction of crankshaft defect moieties such as 2,6-hydroxynaphthoic acid copolymerized with hydroxybenzoic acid. While they do not show fully developed crystallinity as evidenced by their intermediate X-ray diffraction pattern, e.g. Figure 2B,[16] they do demonstrate some features of crystallinity, however, in spite of this. These are large crystallites, high degrees of crystallinity, and rotational correlations necessitated by the herringbone packing of adjacent aromatic groups. The melting tran-

[†] Current address: Cryovac-W.R.Grace, via Trento 7, 20017 Passirana di Rho (Milano), Italy.

[‡] Current address: Ausimont, via S. Pietro 50, 20021 Bollate (Milano), Italy.

0024-9297/93/2226-0385$04.00/0

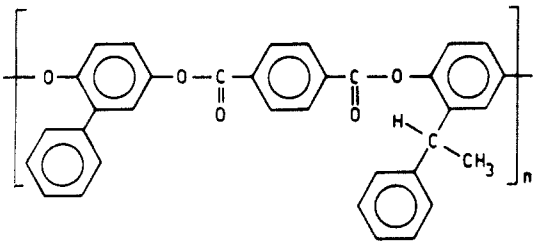

Figure 1. Structure of the copolyester of phenylhydroquinone, phenylethylhydroquinone, and terephthalic acid.

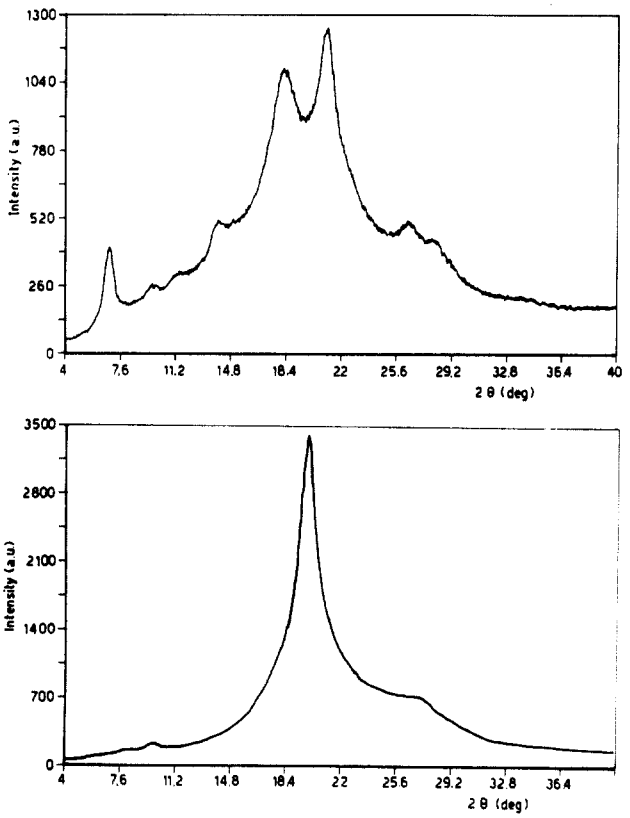

Figure 2. X-ray diffraction patterns for (A, top) the polymer shown in Figure 1 and (B, bottom) the copolymer containing *p*-oxybenzoate and 6-oxy-2-naphthoate units (75/25).

sitions, however, are accompanied by low values of melting enthalpy.

An interesting proposal has been put forth by Windle et al.[17] which may partially describe some of the observed features, inconsistencies, and anomalies of crystallinity in these intermediate cases. The model is one in which small crystallites can be formed or augmented due to fortuitous matching of sequences in parallel nearest neighbor chains. The existence of parallel chains to facilitate crystallization is guaranteed by the nematic state precursor from which the crystallites are formed. The model does not require rotational correlations between adjacent chains and this makes their status as real crystallites dubious. As a consequence these paracrystals give only weak indications by calorimetric or X-ray analysis. Defects in the crystallites arising from sequence mismatch can contribute to X-ray broadening and low values of the melting enthalpy. Polymers of this type show enhanced glass transition strength.

For the purpose of this study the polymer chosen, as exemplified in Figure 1, provides a case for which the crystallization of a rigid molecule from the nematic state with preformed uniaxial order can be observed without the complication of crankshaft defects (in addition to the inherent ester linkages) or flexible spacers, which are often introduced to bring the melting point within a tractable range. One has, thus, in effect a molecular realization of a system which is sufficiently simple so that it could be the subject of calculations, modeling, and testing of theoretical predictions based on a series of simplifying and facilitating assumptions, e.g. rigid rods, uniaxial symmetry, no rotational correlations in the mesophase, and large aspect ratio rods. The large aspect ratio feature of these molecules, i.e. their polymeric nature, could be an important way to test predictions of theories which have heretofore only been subject to evaluation with experimental data for low molar mass compounds.

Experimental Section

The crystallization and melting behavior were studied using a Perkin-Elmer DSC-7 differential scanning calorimeter, DSC, which was calibrated with indium and tin according to ASTM D3417-83. A weighed sample of polymer (8–12 mg) was placed in an aluminum pan and heated at 20 °C/min to 370 °C. The sample was rapidly cooled to a fixed crystallization temperature, T_c, at a nominal rate of 200 °C/min. The heat developed during isothermal crystallization was recorded as a function of time, and the fraction, X, of the crystallizable polymer component converted at time, t, to the crystallized form was evaluated as the ratio of the heat evolved at t over the total heat evolved, i.e. $t \rightarrow \infty$. The $t = 0$ point, t_0, was taken as the deflection point of the exothermal curve from the baseline back-extrapolated after reaching thermal equilibrium. The melting temperatures of isothermally crystallized samples were determined directly heating from T_c at 10 °C/min after the completion of crystallization.

Optical observations were performed using a Leitz Wetzlar optical microscope equipped with a Linkam THM 600 hot stage. Samples were placed between two glass slides and heated at 5–20 °C/min. A Cambridge Stereoscan 604 has been used for performing the scanning electron microscope observations. Samples were prepared by melting 3–5 g of polymer in a silicone oil bath at 370 °C, followed by crystallization under both isothermal and nonisothermal conditions. Isothermal crystallization was performed by quickly transferring melt polymer to a silicone bath kept at constant temperature. The resulting samples were fractured in liquid nitrogen and the fracture surfaces were etched with a 60/40 (w/w) mixture of phenol/tetrachloroethane.

Gel permeation chromatography was performed using a Waters 150-C analyzer equipped with Pl-gel 10 columns using a 50/50 (w/w) mixture of phenol/trichlorobenzene at 85 °C as the solvent.

Materials

The liquid crystalline copolyester as shown schematically in Figure 1 is prepared by the solution polymerization of the acid chloride with the mixture of substituted hydroquinones as described in detail in ref 18. The product is subject to a postpolymerization heat treatment (24 h at 280 °C under nitrogen flow) which results in a molecular weight augmentation. The final product is characterized by inherent viscosity measurements at a concentration of 0.2% (w/v) in a 50/50 (w/w) mixture of phenol/trichlorobenzene at 85 °C. Two samples were chosen for further experimentation and had values which were determined to be 1.26 dL/g for polymer 1 and 1.25 dL/g for polymer 2. Gel permeation chromatography, however, showed polymer 1 to have a bimodal molecular weight distribution with a polydispersity of 3.0, while polymer 2 did not show any bimodality and had a polydispersity of 2.7. Both virgin and melt quenched samples had a glass transition temperature of 134 °C and a specific heat difference at the transition of 0.02–0.05 J/(g °C) as shown by DSC. The melting behavior of the untreated polymers when heated at 20 °C/min showed two endotherms at 310 and 340 °C. Melting to the liquid crystalline nematic phase is accom-

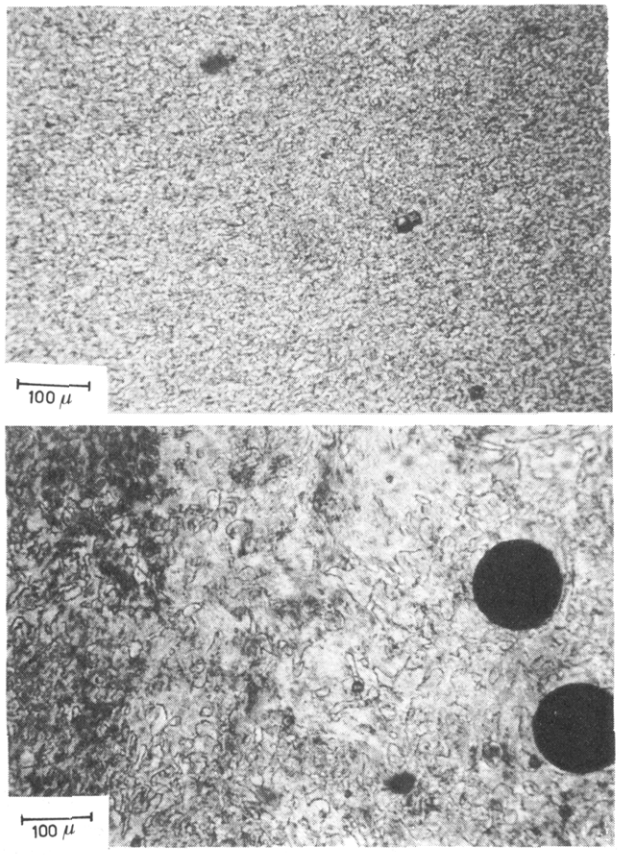

Figure 3. (A, top) A polarized photomicrograph of the birefringent liquid crystalline phase for polymer 2 in excess of 345 °C. (B, bottom) As in A, but reheating the same sample from ambient for a second scan.

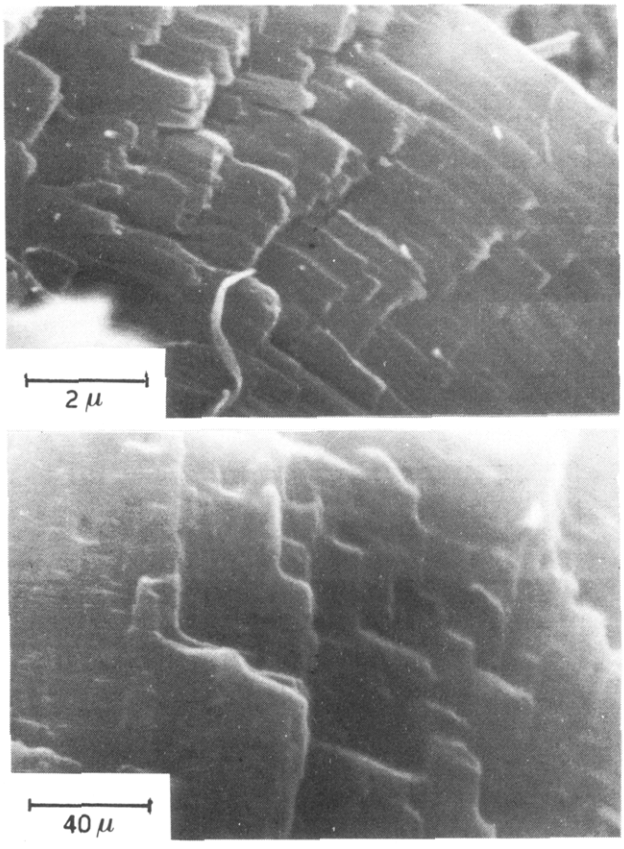

Figure 4. Electron micrograph showing the dependence of morphology on crystallization conditions: (A, top) a microlamellar structure for a sample crystallized under nonisothermal conditions; (B, bottom) increased lamellar dimensions for a sample crystallized slowly under isothermal conditions.

panied by an enthalpic change of 28.5 J/g. The clearing point of the polymers to the isotropic state is obscured by the prior occurrence of thermal decomposition. During cooling at 20 °C/min the polymer shows a single crystallization exotherm at 300 °C accompanied by an enthalpic change of 13 J/g.

Optical microscopy corroborated the results of the DSC experiments and showed the formation of a birefringent liquid phase at 340–345 °C, as shown in Figure 3A, when the sample (polymer 2) was heated at 20 °C/min. A clearing point was not observed as the polymer degraded above 370 °C. On cooling the mesophase at 5 °C/min, the polymer crystallizes at about 300 °C with the retention of microdomains. Reheating at 5 °C/min resulted in a melting temperature at 343 °C with the formation of a typical threaded nematic texture as shown in Figure 3B.

Scanning electron microscopy was performed only on fracture surfaces of samples of polymer 2 crystallized both isothermally and nonisothermally from the melt phase. Figure 4A shows a microlamellar structure for the polymer crystallized nonisothermally by cooling from 370 °C at 20 °C/min. Figure 4B shows the structure of the same sample crystallized isothermally at 320 °C for 30 min after cooling from 370 °C. The lamellae are 2 orders of magnitude larger in the isothermally crystallized sample.

Results and Discussion

The kinetics of the isothermal crystallization from the nematic state of the polymer whose structure is shown in Figure 1 was studied in the temperature range 319–325 °C. The 6 °C interval is dictated by the extremely fast crystallization kinetics which imposes experimental limitations. The heat of crystallization was recorded as a function of time and the primary data, showing the time evolution of the crystallizable component, X, are shown in Figure 5. These data can be interpreted in terms of the rearranged Avrami equation

$$\log(-\ln(1 - X(t))) = \log k + n \log t \qquad (2)$$

for which straight line plots should result in regimes where the Avrami equation is valid, as shown in Figure 6. Deviations from linearity at long times indicate secondary crystallization phenomena which can be quite complicated and obviously not predictable with the simple time dependence contained in the Avrami equation. The existence of secondary crystallization does qualitatively indicate the presence of considerable molecular mobility after the primary event, however.

The Avrami parameters, n, as obtained from the slope of the linear portions of the curves in Figure 6 are shown in Table I. Within experimental error, n is independent of crystallization temperature, T_c, having average values of 2.8 and 2.0 for polymers 1 and 2, respectively. In the first case, the result is consistent with a primary crystallization process resulting from athermal nucleation followed by three-dimensional crystal growth, while in the second case the value of n can be attributed to two-dimensional growth. Note that the latter case suggesting two-dimensional growth is visually confirmed by the occurrence of lamellae in Figure 4. Given the information at hand, this discrepancy must be ascribed to differences in molecular weight distribution for the two samples as previously discussed. Liu and co-workers have recently reported[19] dependence of the growth morphology parameter, n, on molecular weight. The crystallization rate constants, k, as calculated from eq 2 and Figure 6, are also

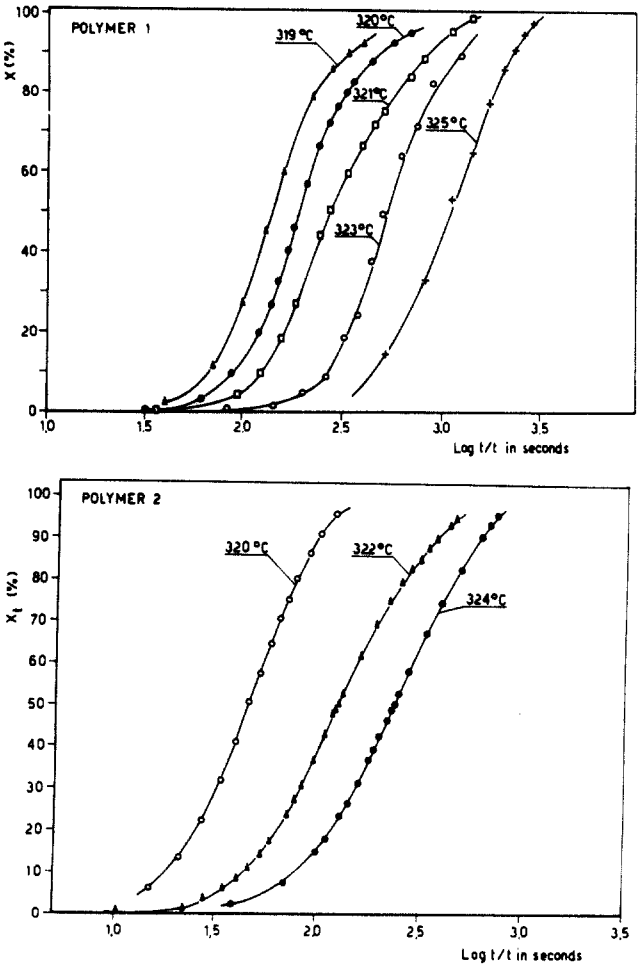

Figure 5. Evolution of the crystalline component, X, upon isothermal crystallization when plotted in terms of the logarithm of time, t, where t is an induction time: (A, top) polymer 1; (B, bottom) polymer 2.

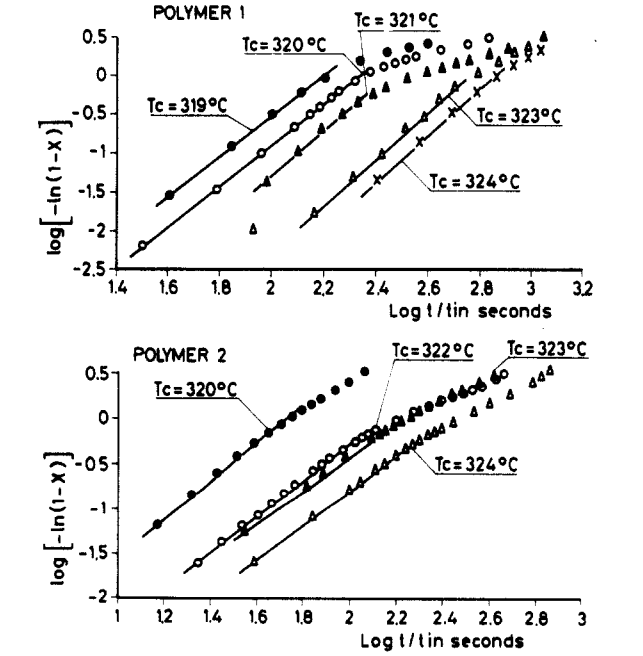

Figure 6. Primary data of Figure 5 plotted according to the rearranged Avrami equation, eq 2, for (A) polymer 1 and (B) polymer 2.

tabulated in Table I. k is found to decrease with increasing T_c; i.e. crystallization becomes slower as the degree of supercooling is diminished. This dependance is more pronounced in polymer 1 where the rate changes by 2 orders

Table I
Kinetic Parameters for Isothermal Crystallization from the Nematic Phase

	polymer 1		polymer 2	
T_c (°C)	n	k (s^{-n})	n	k (s^{-n})
319	2.6	2.18×10^{-6}		
320	2.6	7.13×10^{-7}	2.1	2.45×10^{-4}
321	2.8	1.28×10^{-7}		
322	2.6	1.23×10^{-7}	2.0	6.42×10^{-5}
323	3.0	5.62×10^{-9}	1.8	1.21×10^{-4}
324	2.9	3.20×10^{-9}	1.9	2.57×10^{-5}
av	2.8		2.0	

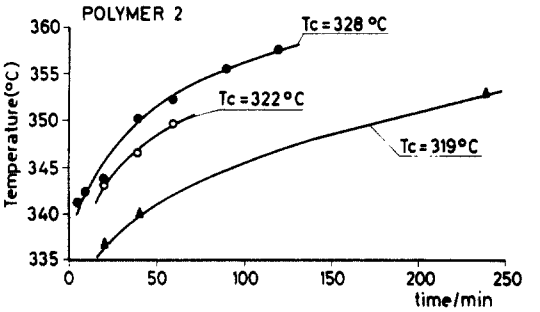

Figure 7. Dependence of the high temperature melting endotherm of polymer 2 on crystallization time for different isothermal crystallization temperatures.

of magnitude for an interval of 5 °C. Again discrepancies between polymer 1 and polymer 2 must be ascribed to differences in molecular weight distribution. Variations in the overall rate constant, k, can be related to both growth rate and nucleation density effects. Since the chains are rigid rods, crystallizing from the nematic state, the crystal morphology is preformed and thus one expects that the parameters obtained contain only a minimal contribution from chain dynamics. Unfortunately, microscopic observations cannot furnish any information regarding the nucleation density because of the difficulty in detecting the presence of crystallites in the birefringent mesophasic fluid.

Melting behavior is strongly dependent on isothermal crystallization time as demonstrated by heating samples of polymer 2 at 10 °C/min in the DSC after completion of the crystallization. Samples crystallized at temperatures lower than 320 °C melt with a single endotherm in all cases, while those crystallized at higher temperatures have double peaks if the crystallization time is greater than 20 min. The fact that Cheng et al.[12] observed double peaks in all cases, with crystallization temperatures as low as 260 °C presumably can be attributed to effects of varying molecular weights and distributions for different samples as noted above. Cheng et al. attributed this second peak to a more stable crystalline polymorph which interconverts from the crystallite formed originally. While both peaks are shifted to higher temperature with increasing crystallization time, the shift in the high temperature peak is most pronounced. Figure 7 shows the crystallization–time dependence of the high temperature peak as a function of T_c. Primary crystallization is completed in 53 s at 320 °C and in 200 s at 324 °C as seen in Figure 6B. Subsequently, overlapping secondary crystallization and annealing processes commence, leading to the formation of high melting crystals. The tendency to perfect the crystalline phase is shown in Figure 8, where the overall increase in melt enthalpy can be seen. At the same time the melting enthalpy in the high temperature peak is seen to grow at the expense of the low temperature peak, indicating a crystal–crystal transition. This behavior appears to be opposed to that observed by Cheng et al. in ref 12. We

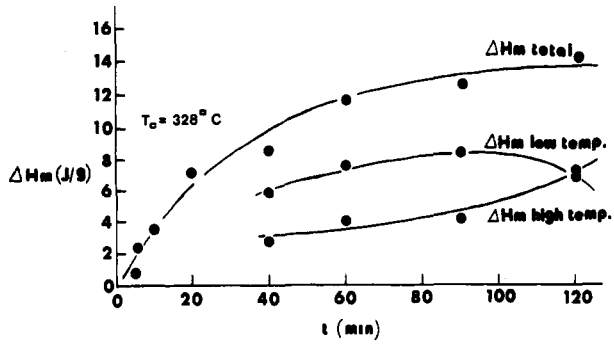

Figure 8. Perfection of crystallites on annealing as evidenced by the melting enthalpy of the component peaks as contrasted to the total melting enthalpy.

Table II
Dependence of Melting Temperature, Enthalpy and Entropy of Melting of Crystallization Temperature for Isothermally Crystallized Samples of Polymer 2

T_c (K)	T_m (K)	H_m (J/g)	S_m (J/(g K))
593	606.9, 612.2	10.9[a]	0.018[b]
595	608.0[c]	10.7	0.018
596	608.9	9.5	0.016
597	609.0	8.6	0.014

[a] First peak, 8.5 J/g; second peak, 2.4 J/g. [b] First peak, 0.014 J/(g K); second peak, 0.004 J/(g K). [c] Shoulder at 611.9 K.

are not in position to explain such a trend; we can only observe that these authors carried out the crystallization experiments at lower temperatures (303 °C being the highest one), obtaining also very different Avrami indices. That clearly means that very different crystallization processes take place in the two cases. Since the sole difference in T_c does not account for such different behavior, differences in the starting samples and in nucleation mechanisms should be considered.

The perfection of crystalline structure during annealing moreover depends on annealing temperature. Similar behavior has been observed in the case of Vectra A900 liquid crystal polymer of the Hoechst-Celanese Corp.[20] Thermal history effects, thus, preclude a discussion of a polymer melting point in the abstract. Furthermore, molecular weight build up by chain extension during the annealing process cannot be ruled out.

The observed melting temperature, T_m, can be used to obtain the equilibrium melting temperature, T_{m_0}, according to the Hoffmann–Weeks method,[21] by extrapolating the curve relating T_m to the crystallization temperature, T_c

$$T_m = ((a-1)/a)T_{m_0} + (T_c/a) \quad (3)$$

to intersect the straight line $T_m = T_c$. This intersection is T_{m_0}. a represents the ratio of the average crystal thickness to that of the original nucleus. In this case, the relationship between T_m and T_c is not unique since T_m is a function of the crystallization time. For purposes of the calculation T_m has been taken as the melting temperature of the primary crystals, i.e. that which is obtained by melting isothermally crystallized samples immediately after the time required for primary crystallization. Table II shows the dependence of T_m on T_c. Using these data with eq 3, the value of T_{m_0} is determined to be 352 °C and $a = 1.78$, indicating a thickening of the crystals during the primary crystallization process. Note that the extrapolated value of T_{m_0} should be taken with reservation inasmuch as there is a 25° extrapolation from the T_c values used and T_m often increases sharply with T_c as T_c approaches T_{m_0}.

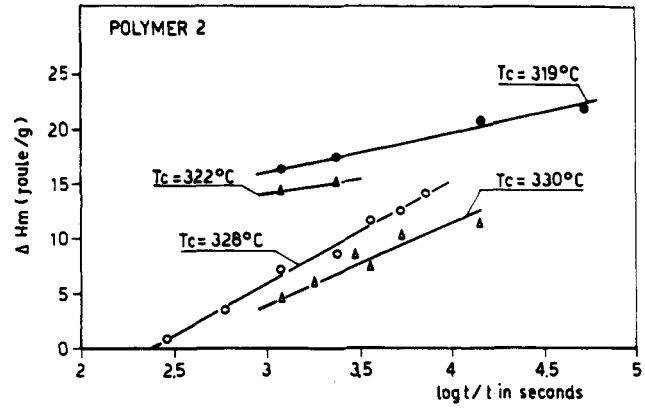

Figure 9. Dependence of melting enthalpy, ΔH_m, of polymer 2 on log t, t being the crystallization time.

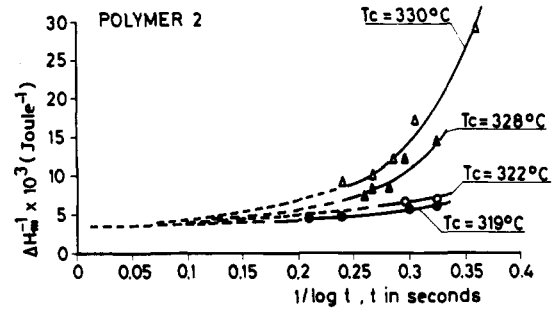

Figure 10. Dependence of reciprocal melting enthalpy, $1/\Delta H_m$, of polymer 2 on $(1/\log t)$ for different isothermal crystallization temperatures, T_c.

The enthalpy of melting also increased with crystallization time. Since a linear relationship was experimentally found between the total melting enthalpy and log t, t being the crystallization time, as shown in Figure 9,[22] the equilibrium melting enthalpy ΔH_{m_0} can be obtained by extrapolating $1/\Delta H_m$ to $1/\log t \rightarrow 0$ as shown in Figure 10. This lengthy extrapolation is quite uncertain, but gives a value of 36 ± 5 J/g comparable to that which has been evaluated from calorimetric observation combined with estimates of percentage crystallinity from X-ray data.

With the above observations being made about features influencing crystallization in rigid rod liquid crystalline polymers, we now try to make some assessments on the effect of the liquid crystalline state on the rates of crystallization. Since the nematic state gives a predisposed chain morphology for the resulting crystallites, one can intuitively imagine that nucleating sites may not be as important for rigid rod polymers as for flexible chain polymers; i.e. the activation barrier may be small. Similarly, motions required of the rigid rod molecules as they crystallize from the nematic state will be limited to rotations around the chain axis and longitudinal displacements of the rod. The rigidity of the rod requires, however, that whole chains be moved into register since the rigid nature of the molecule will limit the importance of the segmental motion. Obviously, if nematic ordering did not exist, the entire process would therefore be much slower. Entanglements then are not an issue. One may expect, therefore, that crystallization of these types of molecules will be rapid, as is indeed the experimental observation. For liquid crystalline polymers, crystallite size can be macroscopic, i.e. the order of the persistence length of the director. For flexible chain polymers, however, segmental motion will dominate the chain dynamics as small crystallites are formed from a multitude of nucleation sites. In assessing the absolute rates of crystallization, one must compare the process for rigid rod liquid crystalline polymers with that of semirigid isotropic polymers, e.g.

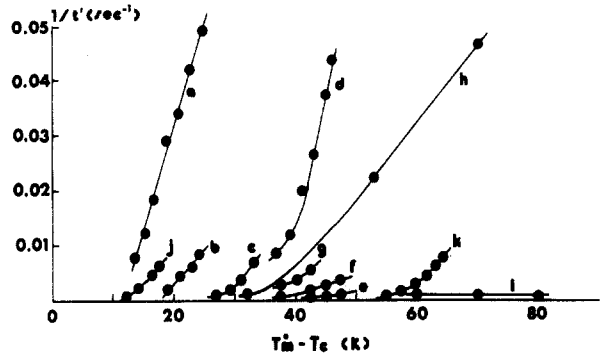

Figure 11. Rate of crystallization, expressed as the reciprocal of the half crystallization time, t' (i.e. the time where the crystallinity is 50% of the total at a given T_c), for various polymers as a function of supercooling $T_{m_0}-T_c$. Symbols and references are given in Table III.

Table III
Explanatory Information for Figure 11

symbol/ abbreviation	structure	ref
a/HTH10	poly(decamethylene-4,4′-terephthaloyl dioxydibenzoate)	10
b/HTH3	poly(trimethylene-4,4′-terephthaloyl dioxydibenzoate)	10
c/this study	Figure 1	
d/PBT	poly(butylene terephthalate)	8
e/PPS-H	poly(phenylene sulfide), high molecular weight	23
f/PPS-M	as above, medium molecular weight	23
g/PPS-L	as above, low molecular weight	23
h/PEEK	polyether–ether–ketone	24
i/PC	polycarbonate	25
j/PE	polyethylene	26
k/iPP	polypropylene isotactic	27

polyether–ether–ketone, polycarbonate, etc. on one hand, and flexible chain polymers, e.g. polyethylene, polypropylene etc. on the other. Such comparison is made in Figure 11 where crystallization rate constants for various polymers are considered as a function of supercooling, i.e. the difference between the melting temperature and the crystallization temperature. One can observe that the polymer under study crystallizes from the nematic state with less supercooling than any polymer crystallizing from the isotropic state except for polyethylene. As previously noted, polyethylene has a highly flexible chain for which the rapid segmental mobility obviously dominates the crystallization kinetics. The negative dependence on crystallization rate with supercooling for polycarbonate is attributed to the close proximity of the T_g at 60–80 °C of supercooling. HTH10 and HTH3 are liquid crystalline polymers containing flexible spacers consisting of 10 and 3 methylene groups, respectively, and crystallize from the smectic phase. The very rapid rate of crystallization for small degrees of supercooling for HTH10 even surpassing the crystallizability of polyethylene indicates that this polymer can crystallize under the combined beneficial influence of the morphological predisposition imparted by the liquid crystalline phase and the ability to undergo rapid sequential motion imparted by the flexible spacer. Evidently, the reduction in spacer length from 10 to 3 impedes the latter effect, thus making the crystallization process somewhat more sluggish.

Conclusion

The isothermal crystallization process for a highly crystalline rigid rod polymer crystallizing from the nematic phase can be described by the Avrami equation during the early stages of the process. Since the crystal morphology is preformed by virtue of the nematic state, the crystallization kinetics reflect only a minor contribution from chain dynamics; i.e. the melt state precursor is well-defined relative to the resulting crystal. This results in a very rapid rate of crystallization. The rate of crystallization increases with the degree of supercooling. The Avrami index, n, varies between 2.0 and 2.8 evidently dependent on molecular weight distribution. The melting temperature is dependent on isothermal crystallization time indicating that secondary processes are capable of forming more perfect structures and that the melting temperature is related to the thermal history of the sample.

Acknowledgment. The authors thank Himont for permission to publish this work and are grateful to A. Windle for useful discussion.

References and Notes

(1) Price, F. P.; Wendorff, J. H. *J. Phys. Chem.* **1971**, *75*, 2839.
(2) Price, F. P.; Wendorff, J. H. *J. Phys. Chem.* **1971**, *75*, 2849.
(3) Price, F. P.; Wendorff, J. H. *J. Phys. Chem.* **1972**, *76*, 276.
(4) Jabarin, S. A.; Stein, R. S. *J. Phys. Chem.* **1973**, *77*, 409.
(5) Price, F. P.; Fritzche, A. K. *J. Phys. Chem.* **1973**, *77*, 396.
(6) Papkov, V. S.; Svitsunov, V. S.; Godowsky, Yu. K.; Zhdanov, A. A. *J. Polym. Sci., Polym. Phys. Ed.* **1987**, *25*, 1859.
(7) Batthacharya, S. K.; Misra, A.; Stein, R. S.; Lenz, R. W.; Hahn, P. E. *Polym. Bull.* **1986**, *16*, 465.
(8) Pracella, M.; Chiellini, E.; Dainelli, D. *Makromol. Chem.* **1989**, *190*, 175.
(9) Avrami, M. *J. Chem. Phys.* **1941**, *9*, 177.
(10) Pracella, M.; Frosini, V.; Galli, G.; Chiellini, E. *Mol. Cryst. Liq. Cryst.* **1984**, *113*, 201.
(11) Grebowicz, J.; Wunderlich, B. *J. Polym. Sci., Polym. Phys. Ed.* **1983**, *21*, 141.
(12) Cheng, S. D. Z.; Zhang, A.; Johnson, R. L.; Wu, Z. *Macromolecules* **1990**, *23*, 1196.
(13) Warner, S. B.; Jaffe, M. *J. Cryst. Growth* **1980**, *48*, 184.
(14) Hong, S. K.; Blackwell, J. *Polymer* **1989**, *30*, 780.
(15) Cheng, S. D. Z.; Johnson, R. L.; Wu, Z.; Wu, H. H. *Macromolecules* **1991**, *24*, 150.
(16) A sample provided by Hoechst-Celanese through the IUPAC working party on liquid crystalline polymers containing *p*-hydroxybenzoic acid/2,6-hydroxynaphthoic acid in a molar ratio of 75/25.
(17) (a) Hanna, S.; Windle, A. H. *Polymer* **1988**, *29*, 207. (b) Golombok, R.; Hanna, S.; Windle, A. H. *Mol. Cryst. Liq. Cryst.* **1988**, *55*, 281.
(18) Lee, D. M.; Hutchings, D. A.; Sieloff, G. M.; Willard, G. F. U.S. Patent 4,600,765, 1984.
(19) Liu, X.; Hu, S.; Shi, L.; Xu, M.; Zhou, Q.; Duan, X. *Polymer* **1989**, *30*, 273.
(20) Lin, Y. G.; Winter, H. H. *Macromolecules* **1988**, *21*, 2439.
(21) Hoffmann, J. D.; Lauritzen, J. I., Jr.; Passaglia, E.; Ross, G. S.; Frolen, L.; Weeks, J. J. *Kolloid Z. Z. Polym.* **1969**, *231*, 564.
(22) Cheng, S. *Macromolecules* **1988**, *21*, 2475.
(23) Song, S. S.; White, J. L.; Chakmak, M. *Polym. Eng. Sci.* **1990**, *30*, 944.
(24) Blundell, D. J.; Osborn, B. N. *Polymer* **1983**, *24*, 953.
(25) Onu, A.; Legras, R.; Mercier, J. P. *J. Polym. Sci., Polym. Phys. Ed.* **1976**, *14*, 1187.
(26) Hay, J. N.; Mills, P. J. *Polymer* **1982**, *23*, 1380.
(27) Crispino, L.; Martuscelli, E.; Pracella, M. *Makromol. Chem.* **1980**, *181*, 1747.

Registry No. (2,5-$(OH)_2C_6H_3Ph$)(2,5-$(OH)_2C_6H_3(CH_2)_2Ph$)-(1,4-$(CO_2H)_2C_6H_4$) (copolymer), 135208-02-5.